Statistical modeling of chikungunya virus intra-vector infection dynamics in a French *Aedes albopictus* population reveals an explosive epidemic potential

Barbara Viginier[1], Céline Garnier[1], Lucie Cappuccio[1], Edwige Martin[2], Claire Valiente Moro[2], Albin Fontaine[3,4,5], Sébastian Lequime[6], Frédérick Arnaud[1], Maxime Ratinier[1], Vincent Raquin[1]

[1] École Pratique des Hautes Études (EPHE), Institut National de la Recherche Agronomique (INRA), Université de Lyon, Université Claude Bernard Lyon1, UMR 754, Infections Virales et Pathologie Comparée (IVPC), Paris Sciences Lettres (PSL) Research University, F-69007, Lyon, France.

[2] Univ Lyon, Université Claude Bernard Lyon 1, CNRS, INRAE, VetAgro Sup, UMR Ecologie Microbienne, F-69622 Villeurbanne, France.

[3] Unité Parasitologie et Entomologie, Département Microbiologie et maladies infectieuses, Institut de Recherche Biomédicale des Armées (IRBA), Marseille, France.

[4] Aix Marseille Univ, IRD, SSA, AP-HM, UMR Vecteurs–Infections Tropicales et Méditerranéennes (VITROME), Marseille, France.

[5] IHU Méditerranée Infection, Marseille, France.

[6] Cluster of Microbial Ecology, Groningen Institute for Evolutionary Life Sciences, University of Groningen, Groningen, The Netherlands.

Keywords : Arbovirus ; vector ; mosquito ; *Aedes albopictus* ; chikungunya virus ; epidemiology ; vector competence

Abstract

Arbovirus emergence and epidemic potential, as approximated by the vectorial capacity formula, depends on several host and vector parameters including vector intrinsic ability to transmit the pathogen. Such ability, called vector competence is influenced by biotic (*e.g.* virus and vector genotype) and abiotic (*e.g.* temperature). Vector competence is often evaluated as a qualitative phenotype although it is a multistep, time-dependent, quantitative phenotype. Combination of experimental and modelling approaches can i) capture intra-vector dynamics of arboviral infection and ii) use data to estimate arbovirus epidemic potential. Here, we measured individual *Aedes albopictus* (Lyon, France) mosquitoes infection, dissemination, and transmission rate upon oral exposure to chikungunya virus (CHIKV, La Reunion Island isolate) at eleven time-points from day 2 to day 20 post-exposure (dpe) for a range of CHIKV infectious doses spanning human viremia. Statistical modelisation indicates an explosive CHIKV intra-vector dynamics mainly due to an absence of dissemination barrier with 100% of the infected mosquitoes ultimately exhibiting a disseminated infection regardless of the viral dose. Transmission rate data revealed a time and dose-dependent but overall weak transmission barrier with individuals transmitting as soon as 2 dpe and >50% infectious mosquitoes at 6 dpe for the highest dose. Epidemiological simulations conducted with an Agent-Based Model based on experimental intra-vector dynamics data showed that even at low mosquito biting rates, CHIKV triggers explosive outbreaks. Together, this reveals the high epidemic potential of this CHIKV isolate with this French metropolitan population of *Aedes albopictus*.

Introduction

Arthropod-borne viruses (arboviruses) are viruses transmitted to vertebrate hosts by blood-sucking arthropods. Dengue virus (DENV), yellow fever virus (YFV), Zika virus (ZIKV) and chikungunya virus (CHIKV) are mosquito-borne viruses of major public health importance, causing hundreds of millions of human infections each year worldwide associated with serious morbidity and mortality (Labeaud, Bashir & King, 2011; Bhatt et al., 2013). These viruses are primarily transmitted to humans by *Aedes aegypti* mosquitoes, although *Aedes albopictus* is often incriminated as a vector. These two vector species expand their native range to spread worldwide, putting half of the world's population at risk of arbovirus transmission (Kraemer et al., 2019). Globalization and urbanization are two identified factors that promote arbovirus emergence by gathering hosts, pathogens and vectors together (Gubler, 2011; Grubaugh et al., 2019). Arbovirus spread is a multi-factorial, dynamic process that can be estimated using the vectorial capacity (Vcap) model, that aims to determine the average number of infectious vector bites that arise per day from one infected host in a susceptible human population (Smith et al., 2012). The vector-centric component of VCap integrates mosquito ecological (density per host, survival) and behavioural (daily biting rate per human) factors along with mosquito-arbovirus interaction factors, namely vector competence (VComp) and extrinsic incubation period (EIP). VComp represents the ability of a mosquito, following an infectious blood meal, to develop midgut infection, disseminate the virus beyond the midgut barrier and subsequently retransmit the virus through the saliva during the next bite. According to the literature, VComp is impacted by biotic (mosquito genotype, virus genotype, virus dose…) and abiotic (temperature, …) factors (Viglietta et al., 2021). VComp is often expressed as qualitative phenotype based on the proportion of infected, disseminated or, less frequently infectious mosquitoes at limited number (~1 to 3) of discrete time points. However, the dynamics of vector competence heterogeneity remains often masked, requiring modeling tools unveil it (Christofferson & Mores, 2011). Arbovirus transmission dynamics is shaped by the distribution of EIPs, the time required for the vector to become infectious. Such distribution can be implemented into epidemiological simulations together with other vectorial capacity estimates in order to capture arbovirus epidemic potential. Recently, ZIKV intra-vector dynamics was modelled highlighting its low epidemic potential in *Aedes albopictus* (Lequime et al., 2020b).

The Asian tiger mosquito, *Ae. albopictus*, is an invasive species that spread worldwide, its current distribution being likely to increase during the next 30 years partly due to urbanization and climate change (Kraemer et al., 2019). Arbovirus detection in field-collected specimens coupled to vector competence laboratory experiments support the permissiveness of the Asian tiger mosquito to numerous arboviruses (Gratz, 2004; Paupy et al., 2009). *Ae. albopictus* in an anthropophagous species (Fikrig & Harrington, 2021), with a trend to take several consecutive blood meals (Delatte et al., 2010) thereby increasing risk of pathogen transmission (Armstrong et al., 2019). Therefore, *Ae. albopictus* must be considered an important arbovirus notably in Europe, where it was designated as the primary vector during autochthonous circulation of DENV and CHIKV in Italy (Rezza et al., 2007; Venturi et al., 2017), Spain (Aranda et al., 2018) and mainland France (Delisle et al., 2015; Succo et al., 2016). As demonstrated for *Ae. aegypti* and DENV (Lambrechts, 2011), *Ae. albopictus* vector competence for CHIKV depends on the complex interaction between mosquito genotype, virus genotype and

environmental conditions (Zouache et al., 2014). The CHIKV 06.21 genotype (East-Central-South African lineage) from La Réunion outbreak in 2006 (Schuffenecker et al., 2006) is considered highly infectious for *Ae. albopictus* in several mosquito populations (Vazeille et al., 2007; Sanchez-Vargas et al., 2019). This isolate was found in mosquito saliva as soon as 2 days post exposure to an infectious blood meal (Dubrulle et al., 2009), in line with the presence of an A226V mutation in the viral E1 envelop gene that promotes virus dissemination in *Ae. albopictus* (Tsetsarkin et al., 2007). However, simultaneous testing of multiple *Ae. albopictus* populations for CHIKV 06.21 within a single vector competence assay underlined population-specific transmission (Vega-Rua et al., 2013, 2014). Several introductions events occurred leading to genetically diverse populations (Sherpa et al., 2019). A French *Ae. albopictus* population (Bar-sur-Loup, Alpes-Maritimes) was experimentally shown to transmit CHIKV 06.21 (Vega-Rua et al., 2013) and CHIKV isolates carrying the A226V mutation were identified in autochthonous human cases in France (Delisle et al., 2015; Calba et al., 2017), underlying a local emergence potential. Few studies explored the impact of intra-vector viral dynamics on arbovirus transmission although prior modelisation of CHIKV EIP found, based on literature data, that the 1-3 days average EIP was substantially overestimated for CHIKV 06.21-*Ae. albopictus* pair, this value being more ~8 days at the earliest (Christofferson et al., 2014). This gap might be at least partly explained by the virus dose, as it positively correlates with *Ae. albopictus* infection rate for CHIKV (Hurk et al., 2010) and could impact dissemination or transmission dynamics. In this context, measuring CHIKV intra-vector dynamics in *Ae. albopictus* upon a range of virus doses and how it influence CHIKV epidemic potential would help to better understand, anticipate and prevent disease emergence.

Here, we modelled the intra-vector dynamics of CHIKV 06.21 in a field-derived population of *Ae. albopictus* from France (Lyon city) according to human viremia related virus doses in the blood meal. After estimating CHIKV viremia range in human blood based on literature data, we exposed *Ae. albopictus* mosquitoes to various doses representative of viral load in human blood. Individual mosquitoes were analysed from day 2 to day 20 post-exposure to CHIKV to determine infection, dissemination and transmission rates. This allowed us to model a dose-dependent intra-vector dynamics, to estimate the strength of vector infection, dissemination and transmission barriers and to access to the distribution of EIP according to the virus dose in the blood meal. These data were implemented in the agent-based model Nosoi (Lequime et al., 2020a) to estimate, using realistic vectorial capacity parameters, the epidemic potential of CHIKV in a French population of *Ae. albopictus*.

Materials and methods

Modeling chikungunya viremia in human

CHIKV RNA load in human blood along the course of infection in symptomatic patients were recovered from two studies. The first study monitored blood CHIKV viremia from a retrospective cohort of 102 febrile patients in Bandung, West Java, Indonesia between 2005 and 2009 (Riswari et al., 2015). The second study assessed CHIKV RNA viremic profile from 36 sera from day 1 to day 7 of illness during a CHIKV epidemic in 2009 in Thepa and Chana districts of Songkhla province, Thailand (Appassakij et al., 2013). For the second study, the blood CHIKV RNA load from individual patients was

not available therefore the median value was used. The viremia quantity data from RT-PCR was expressed on the logarithmic scale to the base 10 before the model fitting. The Wood's gamma-type function was used to model the viremia dynamic. The function is given in equation:

$$y(t) = at^b e^{-ct}$$

where *y(t)* represents the level of viremia in the blood at *t* days post infection, with *a*, *b* and *c* representing constants linked to the viremia dynamic (Islam et al., 2013). Viremia data were originally expressed in time pre- or post- symptom onset while the model represent viremia as a function of time post infection. A fixed arbitrary median intrinsic incubation period of 6 days was added to each viremia time to standardize the time scale between the data and the model. This fixed incubation period falls into the estimated 2-10 days incubation range (Moloney et al., 2014) and was chosen to ensure that all observed viremia data occurred after infection. The model was fitted to the data using non-linear least-squares regression implemented in the *nls* function in the R environment (https://www.R-project.org/). Using this method, a possible intra-human CHIKV viremia dynamic with 95% confidence intervals was proposed.

Chikungunya virus production and titration

The chikungunya virus (CHIKV) strain 06.21 from Indian Ocean lineage was isolated from a new-born serum sample with neonatal encephalopathy in La Réunion island, in 2005 (Schuffenecker et al., 2006). This highly passaged strain was amplified in *Aedes albopictus* cell line C6/36 as described (Raquin et al., 2015). CHIKV was inoculated at a multiplicity of infection of 0.01 on C6/36 cells in Leibovitz's L-15 media (Gibco) with 10% (vol:vol) 1X Tryptose Phosphate Broth (Gibco), 10% (vol:vol) foetal bovine serum and 0.1% (vol:vol) 10,000 Units/mL penicillin/streptomycin (Gibco). Cells were incubated for 3 days at 28°C before the supernatant was clarified by centrifugation for 5 min at 500 G and stored at -80°C as aliquots. CHIKV infectious titer was measured on C6/36 cells using fluorescent focus assay (Raquin et al., 2015). Briefly, 3 x 10^5 cells/well were inoculated in 96-well plates with 40 µL/well of viral inoculum after culture media removal and incubated for 1 h at 28°C. 150 µL/well of a mix 1:1 L-15 media and 3.2% medium viscosity carboxymethyl cellulose (Sigma) were added as an overlay prior to incubate the cells for 3 days at 28°C. After incubation, cells were fixed in 100 µL/well of 4% paraformaldehyde for 20 min then rinsed 3 times in 100 µL/well of 1X Dulbecco's phosphate buffered saline (DPBS) (Gibco) prior to immune labelling. Cells were permeabilized for 30 min in 50 µL/well of 0.3% (vol:vol) Triton X-100 (Sigma) in 1X DPBS + 1% Bovine Serum Albumin (BSA, Sigma) at room temperature then rinsed 3 times in 100 µL/well of 1X DPBS. A Semliki Forest virus anticapsid antibody diluted 1:600 in 1X DPBS + 1% Bovine Serum Albumin (BSA, Sigma) was used as a primary antibody. Cells were incubated in 40 µL/well of primary antibody for 1 h at 37°C, rinsed 3 times in 100 µL/well of 1X DPBS then incubated in 40 µL/well of anti-mouse Alexa488 secondary antibody (Life Technologies) at 1:500 in 1X DPBS + 1% BSA for 30 min at 37°C. Cells were rinsed 3 times in 100 µL/well 1X DPBS then once in 100 µL/well tap water, stored at 4°C overnight prior to plate reading under Zeiss Colibri 7 fluorescence microscope at 10X objective. Plates were stored at 4°C protected from light. Infectious titer of the CHIVK 06.21 stock was 4.25 x 10^8 fluorescent focus unit (FFU) per mL.

Mosquito colony

A French population of *Aedes* (*Stegomyia*) *albopictus* (Skuse, 1895) was used in this study. Mosquito larvae were collected in 2018 in breeding sites from three different sites around Lyon (Rhône, France). The population was maintained and amplified under standard laboratory conditions (28°C, 80% relative humidity, 16:8 hours light:dark cycle) using mice feeding for 10 generations (F_{10}) prior to experiments. Eggs were hatched for 1 h in dechlorinated tap water and larvae were reared at 26°C (16:8 h light:dark cycle) at a density of 200 larvae in 23 x 34 x 7 cm plastic trays (Gilac) in 1.5 L of dechlorinated tap water supplemented with 0.1 g of a 3:1 (TetraMin tropical fish food:Biover yeast) powder every two days. Adults were maintained in 32.5 x 32.5 x 32.5 cm cages (Bugdorm) at 28°C, 80% relative humidity, 16:8 h light:dark cycle with permanent access to 10% sugar solution.

Experimental mosquito exposure to CHIKV

Four to 8-day old females were confined in 136 x 81 mm plastic feeding boxes (Corning-Gosselin) with ~60 females per box. Females were transferred in the level 3 biosafety facility (SFR AniRA, Lyon Gerland) at 26°C, 12:12 h light:dark cycle with no access to sugar solution 16 h before the infectious blood meal. The blood meal was composed of a 2:1 (vol:vol) mixture of washed human erythrocytes (multiple anonymous donors, EFS AURA, CODECOH DC-2019-3507) and viral suspension supplemented with 2% (vol:vol) of 0.5 M ATP, pH 7 in water (Sigma). Feeders (Hemotek) were covered with pig small intestine and filled with 3 mL of infectious blood mixture. Females were allowed to feed for 1h at 26°C and blood aliquots were taken before (T0) and after (1h) the feeding and stored at -80°C for further titration (Figure S1). Mosquitoes were anesthetized on ice and fully engorged females were transferred in 1-pint cardboard containers (10-25 females/container) and maintained with 10% sucrose. Cardboard containers were placed in 18 x 18 x 18 inches cages (BioQuip) and kept in climatic chambers at 26°C, 70% humidity.

Mosquito collection and CHIKV detection

Individual mosquitoes were harvested between day 2 and day 20 post-exposure (dpe) to CHIKV. Saliva was collected first then head and bodies were recovered. Prior to saliva collection, mosquitoes were anesthetized on ice then legs and wings were removed under a stereomicroscope. Individuals were placed on plastic plate maintained by double-sided adhesive tape. The proboscis was inserted in a trimmed 10 µL filtered tip containing 10 µL of foetal bovine serum hold above the mosquito by modeling clay (Heitmann et al., 2018). Two µL of 1% pilocarpine hydrochloride (Sigma) supplemented with 0.1% Tween-20 (Sigma) in water were added on the thorax of each mosquito to promote salivation. Mosquitoes were allowed to salivate at 26°C, 80% relative humidity for 1 h. The foetal bovine serum containing the saliva was expelled in an ice-cold tube filled with 150 µL of DMEM media (Gibco) supplemented with antibiotics solution (Amphotericin B 2.5µg/ml, Nystatin 1/100, Gentamicin 50µg/ml, Penicillin 5U/ml and Streptomycin 5µg/ml (Gibco)). Following salivation, the head and the body of each mosquito were separated using a pin holder with a 0.15 mm minutien pins (FST). Heads and bodies were transferred in separate, individual grinding tubes containing 500 µL of DMEM supplemented with antibiotics (see above) and one 3-mm diameter tungsten bead (Qiagen). Samples were grinded on a 96-well adapter set for 2 x 1 min, 30 Hz using a TissueLyser (Qiagen) then stored at -80°C. CHIKV

detection was performed once on 40 to 50 µL of undiluted (raw) saliva, head and body sample using fluorescent focus assay (see above). Each mosquito sample was declared positive or negative for CHIKV in presence or absence of fluorescent signal, respectively. CHIKV prevalence was calculated as the proportion (in %) of mosquito samples (body, head or saliva) positive for virus signal. Each 96-well plate harboured positive (CHIKV viral stock) and negative (raw grinding media) controls. No signal was detected in negative controls and positive control wells were fully positive for CHIKV signal. Each plate was examined by two independent persons. Of note, saliva samples were deposited immediately (no freezing) on C6/36 cells in order to maximise CHIKV detection notably in samples with low viral load. 30 µL of saliva sample were immediately mixed with 70 µL of TRIzol (Life Technologies) and stored at -80°C prior to RNA isolation. The rest of the samples was stored at -80°C as a back-up.

RNA isolation from saliva

Total RNA was isolated from 30 µL of saliva sample mixed with 70 µL TRIzol and stored at -80°C as described (Raquin et al., 2017). After thawing samples on ice, 20 µL of chloroform (Sigma) were added. The tubes were mixed vigorously, incubated at 4°C for 5 min and centrifuged at 17,000 G for 15 min, 4°C. The upper phase was transferred in a new tube containing 60 µL isopropanol supplemented with 1 µL GlycoBlue (Life Technologies). Samples were mixed vigorously and stored at -80°C overnight to allow RNA precipitation. After 15 min at 17,000 G, 4°C the supernatant was discarded and the blue pellet was rinsed with 500 µL ice-cold 70% ethanol in water. The samples were centrifuged at 17,000 G for 15 min, 4°C, the supernatant was discarded and the RNA pellet was allowed to dry for 10 min at room temperature. Ten µL of RNAse-free water (Gibco) were added and samples were incubated at 37°C for 10 min to solubilize RNA prior to transfer in RNAse-free 96-well plates and storage at -80°C.

CHIKV RNA load quantification

Two µL of total RNA isolated from individual mosquito saliva was used as template in one-step TaqMan RT-qPCR assay. The QuantiTect Virus kit (Qiagen) was used to prepare the reaction mix in a final volume of 30 µL. The reaction solution consisted of 6 µL 5X master mix, 1.5 µL of primers (forward 5'- CCCGGTAAGAGCGGTGAA-3' and reverse 5'-CTTCCGGTATGTCGATGGAGAT-3') and TaqMan probe (5'-6FAM-TGCGCCGTAGGGAACATGCC-BHQ1-3') mix at 0.4 µM and 0.2 µM final concentration respectively, 0.3 µL of 100X RT mix, 20.2 µL of RNAse-free water (Gibco) and 2 µL of template RNA. RT-qPCR reaction was conducted on a Step One Plus machine (Applied) for 20 min at 50°C (RT step), 5 min at 95°C (initial denaturation) and 40 cycles with 15 s at 95°C and 45 s at 60°C. Serial dilutions of CHIKV 06.21 RNA from 1 x 10^8 to 1 x 10^1 copies/µL were used as an external standard curve to allow estimation of CHIKV RNA load in saliva samples. Each plate contained duplicates of standard samples as well as negative controls and random saliva samples without reverse transcriptase (RT-), in duplicate. Samples with a Cq value outside the linear range of the standard curve or higher than the RT- controls were excluded from the analysis. Aliquots from the same standard were used for all the plates, and samples from a single time-point were measured on the same plate to facilitate sample comparison.

243

244 **Statistical analysis**

245 Mosquito infection (number of CHIKV-positive mosquito bodies / number engorged
246 mosquitoes), dissemination (number of CHIKV-positive heads / number of CHIKV-positive bodies),
247 transmission efficiency (number of CHIKV-positive saliva / number engorged mosquitoes) and
248 transmission rate (number of positive CHIKV-saliva / number of CHIKV-positive heads) were analysed
249 by logistical regression and considered as binary response variables. The time (day post-exposure) and
250 virus dose (in $\log_{10}$ FFU/mL) were considered as continuous explanatory variables in a full factorial
251 generalized linear model with a binomial error and a logit link function. Logistic regression assumes a
252 saturation level of 100% and could not be used to model the relationship between the probability of
253 transmission (response variable) and the time post infection, the dose and their interaction (predictors).
254 We first estimated the saturation level (K) for each dose and subtracted the value N= number of
255 mosquito with CHIKV dissemination x (100% - K) to the number of mosquitoes without virus in their
256 saliva at each time post virus exposure to artificially remove mosquitoes that would never ultimately
257 transmit the virus from the dataset. Logistic regression was then used on these transformed data to
258 predict transmission rates across time post virus exposure and the virus oral dose (Figure S2). Statistical
259 significance of the predictors' effects were assessed by comparing nested models using deviance
260 analysis based on a chi-squared distribution. All the statistical analyses were performed under R
261 environment and figures were created with the package ggplot2 within the Tidyverse environment
262 (Wickham et al., 2019).

263

264 **Epidemiological modeling using Nosoi**

265 A series of stochastic agent-based model simulations were performed using the R package
266 Nosoi as described (Lequime et al., 2020b). Briefly, transmission was considered only between infected
267 mosquito and uninfected human, or between an infected human and an uninfected mosquito. Vertical
268 and sexual transmission, and the impact of potential superinfection were ignored during the simulations.
269 We assumed no particular structure within host and vector populations. It was assumed that humans do
270 not die from infection and leave the simulation after they cure from infection (here 12 days). Mosquitoes
271 daily probability of survival was set at 0.85, and human viremic profile followed our modelisation (Figure
272 1). Each human agent experienced a Poisson-like distribution of bites per day with a mean value
273 manually set at 1, 2, 3, 4, 5, 6, 7, 8, 9, 10 or 60 based on field measurement of *Aedes albopictus* blood
274 feeding behaviour (Delatte et al., 2010).

275

276

Results

Estimating CHIKV viremia in human by modelisation of clinical data.

We aimed to provide a realistic dynamic of CHIKV viremia in human based on viral load measured in sera from human cases, despite scarce data from literature. We found two studies (Appassakij et al., 2013; Riswari et al., 2015) providing time course of human CHIKV viremia, resulting in 5 patients from which blood samples were harvested at 3 to 6 different time points prior or post symptoms onset and analysed for viral load (Figure 1A). The CHIKV load ranged from 10^1 to 6.14 x 10^8 PFU equivalent/mL with two patients displaying from 1.1 x 10^1 to 1.79 x 10^3 PFU equivalent/mL prior to symptoms onset. The viremia peak is reached between day 6 and 7 post-infection, corresponding to day 0 and 1 post-symptoms onset and ranges from 1.03 x 10^7 to 6.14 x10^8 PFU equivalent/mL. CHIKV viremia is then rapidly decreasing, ranging at day 10-13 post-infection between 4.3 x 10^1 to 4.05 x 10^2 PFU equivalent/mL. Of note, one patient presented a detectable CHIKV viremia up to day 19 post-infection with a viral load at 10^1 PFU equivalent/mL (Figure 1A). A Wood's gamma-type function was fitted to the data to provide a model describing intra-human CHIKV loads as a function of time post infection.

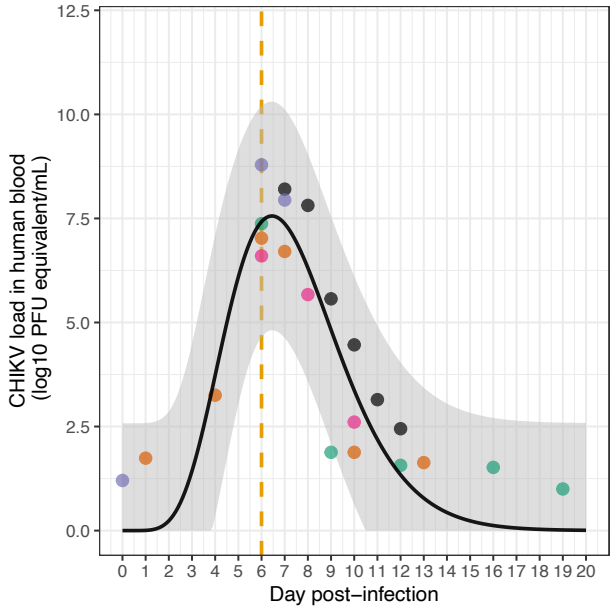

Figure 1. Estimated time course of CHIKV load (in log_{10} PFU equivalent/mL) in human blood as a function of time post infection. A Wood's gamma-type function was used to model CHIKV viremia dynamics based on human viremia data. The black line represents model prediction using mean fit parameter values. Each dot represent a single experimental measurement, dot colors correspond to different patients (*n*=5). The grey ribbon represents upper and lower predicted values.

Ae. albopictus infection rate varies upon virus dose but not time.

Female *Ae. albopictus* from Lyon (France) were exposed to an human erythrocytes suspension containing three doses (8.71 x 10^4, 1.17 x 10^6 and 4.2 x 10^8 FFU/mL) of CHIKV spanning the range of human viremia. Mosquito body infection rate increases with virus dose regardless of the time post-

exposure to CHIKV (Wald Chi-2, P_{dose} = 1.1 x 10^{-6}, P_{time} = 0.9 and $P_{dose*time}$ = 0.17) (Figure 2A). As mosquito body infection rate depends on virus dose but not on time post-exposure, we fitted a logistic model to the data considering CHIKV blood meal titer as unique explanatory variable. A dose of 1.12 x 10^5 FFU/mL is required to infect 25% of the mosquitoes corresponding to the oral infectious dose 25% ($OID_{25\%}$). Mosquito body infection rate variation according to CHIKV oral dose follows a sigmoid pattern, with an $OID_{50\%}$ estimated at 3.98 x 10^5 FFU/mL and an $OID_{75\%}$ corresponding to 1.41 x 10^6 FFU/mL. Within a one log_{10} variation in virus dose (from 1 x 10^5 to1 x 10^6 FFU/mL), mosquito body infection rate jumps from 25 to 75% to reach a plateau at ~100% above 3.16 x 10^7 FFU/mL (Figure 2B).

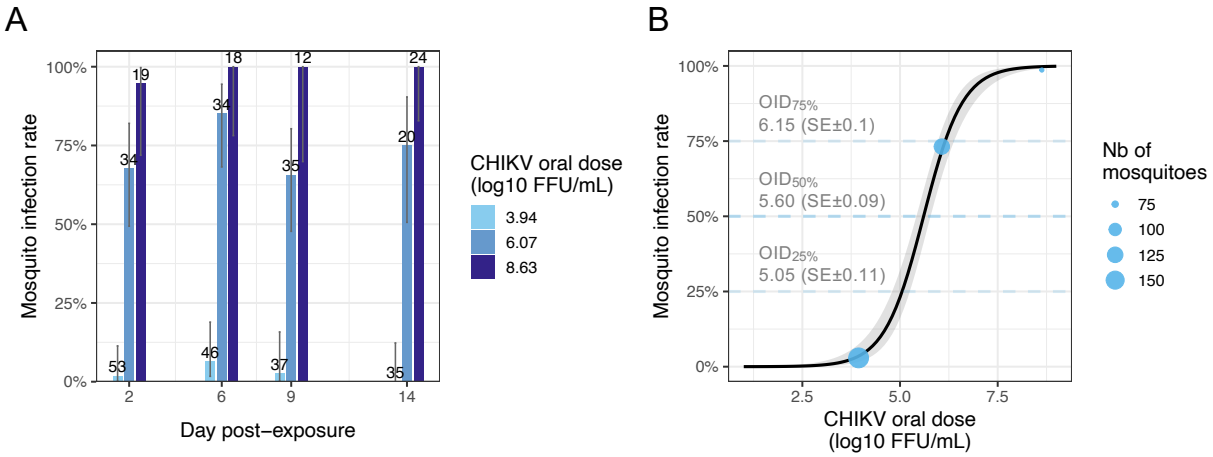

Figure 2. Dose-dependent infection rate of *Ae. albopictus* mosquitoes exposed to CHIKV 06.21. (**A**) Proportion (in %) of *Ae. albopictus* female bodies positive for CHIKV infection (as determined by detection of infectious particles) at four days post-exposure (2, 6, 9 and 14) to three virus doses (8.71 x 10^4, 1.17 x 10^6 and 4.2 x 10^8 FFU/mL) in the blood meal. The number of individual females analysed at each time point is indicated, with the 95% confidence interval associated. (**B**) Mosquito infection rate response to CHIKV dose in the blood meal. Blue dots correspond to the observed infection rate upon each of the three CHIKV oral dose tested. Dot size is proportional to the number of mosquitoes tested. The black line was obtained by fitting a logistic model to the data. The grey ribbon indicates the 95% confidence intervals. The oral infectious dose (OID) to infect 25%, 50% and 75% of the mosquitoes exposed to CHIKV is indicated (in log_{10} FFU/mL) with the associated standard error.

Virus dose and time dependence of *Ae. albopictus* dissemination dynamics.

The proportion of CHIKV positive heads among positive bodies (*i.e.* mosquito dissemination rate) was analysed using virus dose, time post-exposure and their interaction as explanatory variables. Both time and virus dose impact dissemination rate although not in interaction (Wald Chi-2, P_{dose} = 8.29 x 10^{-6}, P_{time} = 1.75 x 10^{-6} and $P_{dose*time}$ = 0.83) (Figure 3A). Data showed that 100% dissemination was reached at dose 8.71 x 10^4 (n=1/1) and dose 4.2 x 10^8 (*n*=18/18) FFU/mL whereas 95.6% dissemination was reached at dose 1.17 x 10^6 FFU/mL (*n*=22/23). For the two highest virus doses, high dissemination values were measured as soon as day 6 (93.1% at dose 1.17 x 10^6 FFU/mL and 100% at dose 4.2 x 10^8 FFU/mL) whereas the maximum dissemination rate (100%) for dose 8.71 x 10^4 FFU/mL was obtained at day 9 post-exposure to CHIKV (Figure 3A). The estimated time to reach 50% dissemination

in *Ae. albopictus* females exposed to CHIKV was 7.5 days, 2.2 days and below 1 day for 8.71 x 10^4, 1.17 x 10^6 and 4.2 x 10^8 FFU/mL CHIKV doses in the blood meal, respectively. Dissemination dynamics within the mosquito vector was inferred from experimental data for a range of CHIKV oral dose from 1 x 10^3 to 1 x 10^8 FFU/mL (Figure 3B). Interestingly, all the CHIKV doses tested led to 100% dissemination within the time range used for predictions (up to 40 days) although it requires a longer time for the lowest virus doses tested. These data indicates that if a dissemination barrier exists in *Ae. albopictus* against CHIKV, it only slow down the dissemination process without preventing all infected mosquitoes to develop a disseminated infection.

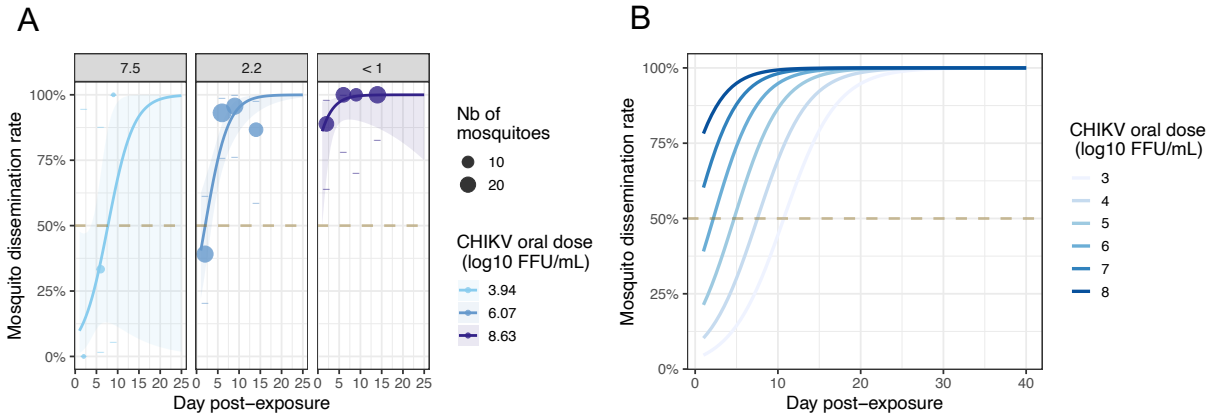

Figure 3. Dose-dependent dissemination rate of *Ae. albopictus* mosquitoes exposed to CHIKV 06.21. (**A**) Mosquito dissemination dynamics. Each dot corresponds to the proportion (in %) of *Ae. albopictus* female heads positive for CHIKV infection (as determined by detection of infectious particles) at four time points (2, 6, 9 and 14 days post-exposure) to three virus doses (8.71 x 10^4, 1.17 x 10^6 and 4.2 x 10^8 FFU/mL) in the blood meal. No disseminated females could be detected at day 14 post-exposure at the lowest CHIKV oral dose (8.71 x 10^4 FFU/mL). Dots size is proportional to the number of mosquitoes tested. Logistic regression was used to model the time-dependent effect of the virus dose on mosquito dissemination rate. Lines correspond to fit values with their 95% confidence intervals displayed as ribbons. The time needed to reach 50% dissemination is 7.5, 2.2 and <1 day for the 8.71 x 10^4, 1.17 x 10^6 and 4.2 x 10^8 FFU/mL CHIKV oral dose, respectively as indicated within each facet label. (**B**) Predicted dissemination dynamics according to virus dose and time post-exposure for a range of CHIKV blood meal titres (1 x 10^3 to 1 x 10^8 FFU/mL).

Time post-exposure impacts CHIKV transmission pattern and saliva viral load.

In the light of previous data, we inferred mosquito transmission dynamics upon various CHIKV oral dose. To that aim, we monitored, at fine time scale, the presence of infectious CHIKV particles in individual mosquito saliva collected by forced salivation technique. This allowed us to measure the dynamics of virus transmission, estimate extrinsic incubation period (EIP) and monitor individual viral load in saliva. Within this experimental design, only two viral doses were tested arbitrarily designed intermediate (4.8 x 10^5 FFU/mL) and high (1.14 x 10^8 FFU/mL) to allow the collection of individual mosquitoes head and saliva at eleven time points (day 2, 3, 4, 5, 6, 7, 10, 12, 14, 17 and 20 post-exposure) that spanned the major part of mosquito expected lifespan. The proportion of CHIKV-positive

saliva among positive bodies (*i.e.* transmission rate) was analysed using virus dose, time post-exposure and their interaction as explanatory variables. Only time impacts transmission rate (Wald Chi-2, P_{time} = 0.0037, P_{dose} = 0.18, and $P_{dose*time}$ = 0.8) (Figure 4A). Infectious saliva samples were detected as soon as day 2 post-exposure to CHIKV, with 33% transmission rate at dose 4.8 x 10^5 FFU/mL (*n*=1/3) and 14% at dose 1.14 x10^8 FFU/mL (*n*=2/14). From day 2 post-exposure, the transmission rate tends to increase following a sigmoid shape, reaching a plateau around 60% for both doses (4.8 x 10^5 and 1.14 x 10^8 FFU/mL) (Figure 4A). The time needed to reach 50% infectious mosquitoes, *i.e.* Extrinsic Incubation Period 50% (EIP_{50}) was 7.5 and 3.5 days for dose 4.8 x 10^5 and 1.14 x 10^8 FFU/mL, respectively. The proportion of mosquitoes that would never ultimately transmit the virus were artificially removed from the dataset based on predicted saturation level at each dose (*ie*. 40% of mosquitoes without virus in their saliva were removed at each time post infection) to ensure a saturation level of 100%, a prerequisite to apply logistic regression analysis on these data. Logistic regression was used on transformed data to predict transmission rates across a range of oral virus doses and times post virus infection. Supplementary figure S2 describes the cumulative proportion of mosquitoes with a systemic infection reaching infectiousness (*i.e.* EIP) over time post infection for a given dose (Figure S2).

We questioned if the amount of CHIKV in the saliva could be associated with the oral dose mosquitoes were challenged with. Total RNA was isolated from individual saliva samples, for the 4.8 x 10^5 and 1.14 x 10^8 FFU/mL doses at each time point, then CHIKV RNA load was measured by TaqMan RT-qPCR assay and analysed according to virus dose and time post-exposure (Figure 4B). Only the time post-exposure had a significant effect indicating an overall decrease of viral load in mosquito saliva over time regardless of the initial dose of exposure despite important inter-individual variations (Anova, P_{time} = 0.006, P_{dose} = 0.66 and $P_{dose*time}$ = 0.94). Of note, when analysing all the saliva positive for CHIKV RNA including samples with no detectable infectious virus, analysis showed that CHIKV RNA load depends both on time post-exposure and, to a lesser extent, virus dose (Anova, P_{time} = 0.047, P_{dose} = 0.01 and $P_{dose*time}$ = 0.77) (Figure S3).

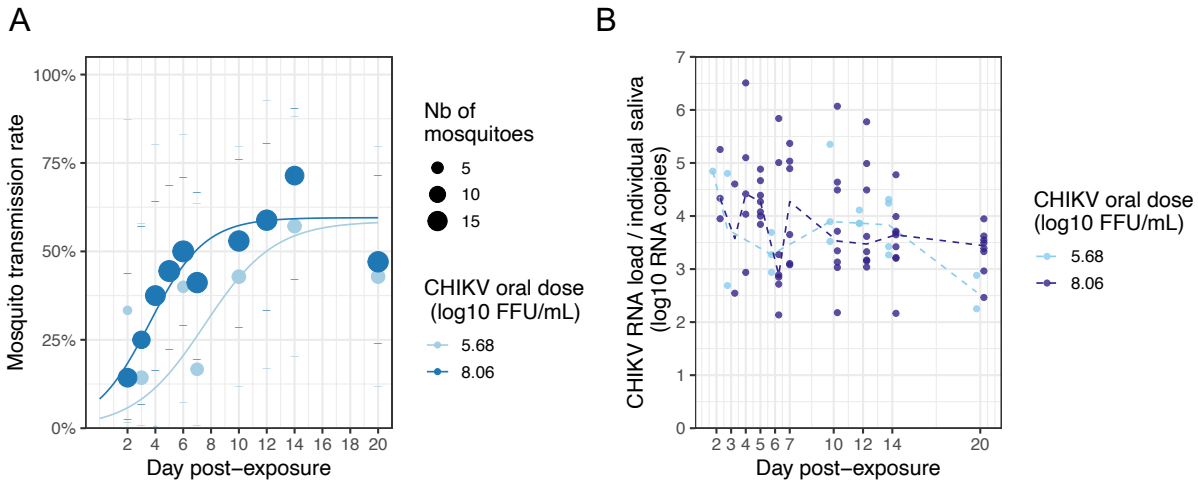

Figure 4. Transmission dynamics of CHIKV 06.21 by *Ae. albopictus*. (**A**) Mosquito transmission dynamics. Each dot corresponds to the proportion (in %) of *Ae. albopictus* female saliva positive for

CHIKV infection (as determined by detection of infectious particles) at ten time points (2, 3, 4, 5 , 6, 7, 10, 12, 14, and 20 days post-exposure) for two virus doses (4.8 x 10^5 and 1.14 x 10^8 FFU/mL) in the blood meal. Dots size is proportional to the number of saliva tested. (**B**) The CHIKV RNA load of each individual saliva scored positive for infectious CHIKV was measured by TaqMan RT-qPCR assay using a synthetic RNA as standard then expressed in $\log_{10}$ RNA copies/saliva. Each dot within represents a saliva sample from an individual mosquito exposed to the indicated CHIKV oral dose (in $\log_{10}$ FFU/mL).

Simulation of CHIKV epidemic upon dose-dependent intra-vector dynamics

A stochastic agent-based model (ABM) was used to assess the epidemiological impact of within-host CHIKV dynamics using the R package Nosoi, as done previously for ZIKV (Lequime et al., 2020b). Starting with one infected human in a population of susceptible humans and mosquitoes, the model simulates CHIKV transmissions according to human viremia and the associated probability of mosquito infection and virus transmission timeliness (EIP). The model was run 100 independent times over 365 days for a range of eleven mean individual mosquito biting rates (1, 2, 3, 4, 5, 6, 7, 8, 9, 10 and 60 independent mosquitoes biting per person per day). Simulations led to a high proportion of sustainable epidemics (>100 secondary infections) even under a low mosquito biting rate (Figure 5).

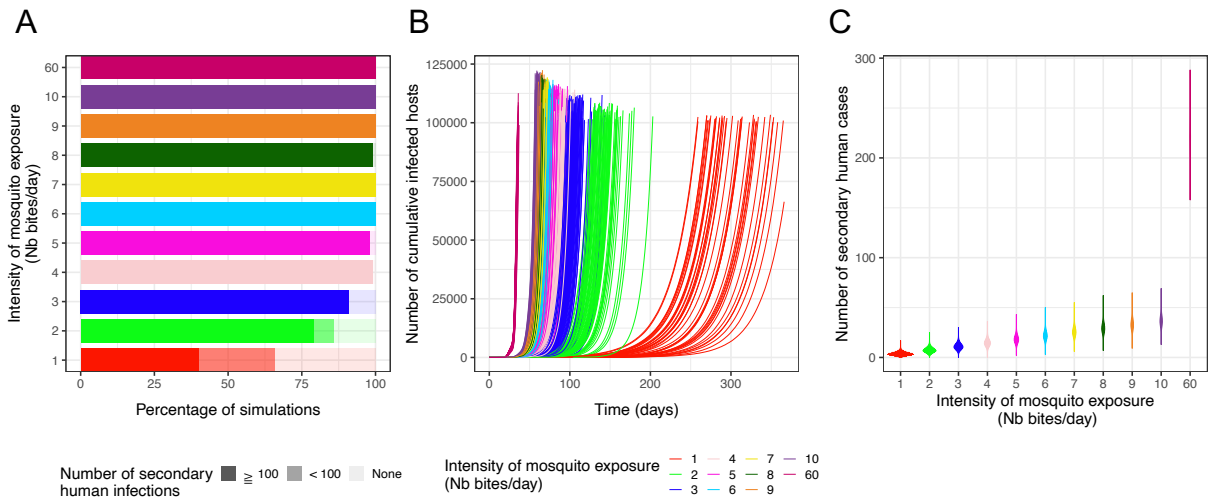

Figure 5. Influence of dose-dependent intra-mosquito CHIKV dynamics on outbreak simulations with various levels of mosquito bites. Stochastic agent-based epidemiological simulations considering within-host infection dynamics on transmission probability during mosquito-human infectious contacts were performed in 100 independent replicates. A total of 11 mosquito bite intensity levels were tested: 1, 2, 3, 4, 5, 6, 7, 8, 9, 10 and 60 bites per human per day. (**A**) Stacked proportions of outbreaks resulting in no secondary infected human host, infected human hosts < 100 and infected human hosts ≧ 100. (**B**) Cumulative number of infected humans over time. Each curve represents a simulation run. (**C**) Violin plots showing the number of secondary cases values densities for each intensity of mosquito exposure.

Discussion

Our work uncovers the intra-vector dynamics of CHIKV in *Ae. albopictus* upon a range of virus doses that are representative of human CHIKV viraemia. Few data are available on the time course of viraemia in individual humans, this parameter being rather determined at a few discrete time-points and often in pooled blood samples. Available studies suggest that human viremia is short (up to 12 days) with viral load ranging from 10^3 to 10^{10} RNA copies / mL, or 10^4 to 10^7 as expressed in PFU/mL (Lanciotti et al., 2007; Laurent et al., 2007; Panning et al., 2008). Our modelisation of human viraemia in blood, although based on limited studies, match these data and also shows a similar pattern to non-human primates in which CHIKV 06.21 viremia last up to 5-7 days post-exposure, with detectable viral RNA at soon as day 1. The CHIKV 06.21 load in the macaques blood ranges between 10^4 to 10^9 viral RNA copies / mL with a peak at day 2 post-exposure (Labadie et al., 2010; Messaoudi et al., 2013). However, our CHIKV viremia modelisation in human blood post infection is not representing the average viremia load post infection in human and is just provided as an example to help the interpretation of CHIKV vector competence data. More individual viremia data, expressed as infectious particles per mL, would be needed to assess an accurate intra human viremia.

Dose-response experiments in mosquitoes confirmed that CHIKV infection initiation in mosquito midgut directly depends on the initial number of viral particles in the blood meal, independently of the time as shown for ZIKV (Lequime et al., 2020b). Interestingly, despite very close infectious dose for 50% of the mosquitoes ($OID_{50\%}$) *i.e.* 5.6 log10 FFU/mL for CHIKV and 5.62 log10 FFU/mL for ZIKV, CHIKV dissemination is more explosive compare to ZIKV (Lequime et al., 2020b). Study of CHIK from Asian lineage in *Ae. aegypti* suggested that viral replication kinetics in the midgut, in link with 3'UTR viral region supports viral dissemination rather than viral load (Merwaiss et al., 2020). In our study, we found that even at the lowest oral dose, that corresponds to a medium-low value in human viraemia, all the individuals presented a disseminated infection. This underscores that the dissemination potential is a key feature for arboviruses that should be carefully characterized. Indeed, this suggest that even a few mosquitoes exposed to low viraemia CHIKV humans will become infected they will transmit the virus. Transmission is usually used as a proxy of viral transmission potential while ignoring the salivary gland infection and escape barrier. To our knowledge, our study is the first to analyse transmission dynamics by scoring individual saliva samples from day 2 to day 20. We found that the saliva barrier was low as ~50% of the mosquitoes were found with at least one viral particle in the saliva from day 6 to day 20 post CHIKV exposure. We also highlighted that transmission was quick, as we detected positive mosquito saliva as soon as day 2 post-exposure (~12%) as previously reported (Dubrulle et al., 2009) although no mosquitoes was collected on the day after virus exposure. A recent study on longitudinal CHIKV expectoration in saliva by *Ae. aegypti* using non-sacrificial method showed an on/off presence of virus in saliva underlying questioning viral persistence in mosquito tissues (Mayton et al., 2021). We uncovered that virus load in individual mosquitoes depends on both time post-exposure and viral dose. It suggests that elder mosquitoes transmitted overall a lower dose, and that the virus dose in the blood meal could influence a global mosquito "infection state" that impacts transmission.

Acknowledgments

469 This project was funded by IDEX Lyon scientific breakthrough project, Micro-Be-Have. We thank all the
470 members from the Micro-Be-Have consortium for insightful discussions. We also thank Dr. Carine
471 Maisse-Paradisi from IVPC unit for the king gift of anti-SVF antibody. We thank Anna-Bella Failloux and
472 Patrick Mavingui for providing the CHIKV 06.21 isolate. Thanks to the managers of the AniRa biosafety
473 level 3 platform under the supervision of SFR biosciences.
474

References

Appassakij H, Khuntikij P, Kemapunmanus M, Wutthanarungsan R, Silpapojakul K. 2013. Viremic profiles in chikv-infected cases. *Transfusion* 53:2567–2574. DOI: 10.1111/j.1537-2995.2012.03960.x.

Aranda C, Martínez MJ, Montalvo T, Eritja R, Navero-Castillejos J, Herreros E, Marqués E, Escosa R, Corbella I, Bigas E, Picart L, Jané M, Barrabeig I, Torner N, Talavera S, Vázquez A, Sánchez-Seco MP, Busquets N. 2018. Arbovirus surveillance: first dengue virus detection in local Aedes albopictus mosquitoes in Europe, Catalonia, Spain, 2015. *Eurosurveillance* 23:1700837. DOI: 10.2807/1560-7917.es.2018.23.47.1700837.

Armstrong PM, Ehrlich HY, Magalhaes T, Miller MR, Conway PJ, Bransfield A, Misencik MJ, Gloria-Soria A, Warren JL, Andreadis TG, Shepard JJ, Foy BD, Pitzer VE, Brackney DE. 2019. Successive blood meals enhance virus dissemination within mosquitoes and increase transmission potential. *Nature microbiology*:1–9. DOI: 10.1038/s41564-019-0619-y.

Bhatt S, Gething PW, Brady OJ, Messina JP, Farlow AW, Moyes CL, Drake JM, Brownstein JS, Hoen AG, Sankoh O, Myers MF, George DB, Jaenisch T, Wint GRW, Simmons CP, Scott TW, Farrar JJ, Hay SI. 2013. The global distribution and burden of dengue. *Nature* 496:504–507. DOI: 10.1038/nature12060.

Calba C, Guerbois-Galla M, Franke F, Jeannin C, Auzet-Caillaud M, Grard G, Pigaglio L, Decoppet A, Weicherding J, Savaill M-C, Munoz-Riviero M, Chaud P, Cadiou B, Ramalli L, Fournier P, Noël H, Lamballerie XD, Paty M-C, Leparc-Goffart I. 2017. Preliminary report of an autochthonous chikungunya outbreak in France, July to September 2017. *Eurosurveillance* 22:17–00647. DOI: 10.2807/1560-7917.es.2017.22.39.17-00647.

Christofferson RC, Chisenhall DM, Wearing HJ, Mores CN. 2014. Chikungunya Viral Fitness Measures within the Vector and Subsequent Transmission Potential. *PLoS ONE* 9:e110538. DOI: 10.1371/journal.pone.0110538.

Christofferson RC, Mores CN. 2011. Estimating the Magnitude and Direction of Altered Arbovirus Transmission Due to Viral Phenotype. *PLoS ONE* 6:e16298. DOI: 10.1371/journal.pone.0016298.

Delatte H, Desvars A, Bouétard A, Bord S, Gimonneau G, Vourc'h G, Fontenille D. 2010. Blood-Feeding Behavior of Aedes albopictus , a Vector of Chikungunya on La Réunion. *Vector-Borne and Zoonotic Diseases* 10:249–258. DOI: 10.1089/vbz.2009.0026.

Delisle E, Rousseau C, Broche B, Leparc-Goffart I, L'Ambert G, Cochet A, Prat C, Foulongne V, Ferré JB, Catelinois O, Flusin O, Tchernonog E, Moussion IE, Wiegandt A, Septfons A, Mendy A, Moyano MB, Laporte L, Maurel J, Jourdain F, Reynes J, Paty MC, Golliot F. 2015. Chikungunya outbreak in Montpellier, France, September to October 2014. *Eurosurveillance* 20. DOI: 10.2807/1560-7917.es2015.20.17.21108.

Dubrulle M, Mousson L, Moutailler S, Vazeille M, Failloux A-B. 2009. Chikungunya virus and Aedes mosquitoes: saliva is infectious as soon as two days after oral infection. *PloS One* 4:e5895. DOI: 10.1371/journal.pone.0005895.

Fikrig K, Harrington LC. 2021. Understanding and interpreting mosquito blood feeding studies: the case of Aedes albopictus. *Trends in Parasitology* 37:959–975. DOI: 10.1016/j.pt.2021.07.013.

Gratz NG. 2004. Critical review of the vector status of Aedes albopictus. *Medical and Veterinary Entomology* 18:215–227. DOI: 10.1111/j.0269-283x.2004.00513.x.

Grubaugh ND, Ladner JT, Lemey P, Pybus OG, Rambaut A, Holmes EC, Andersen KG. 2019. Tracking virus outbreaks in the twenty-first century. *Nature Microbiology* 4:10–19. DOI: 10.1038/s41564-018-0296-2.

517 Gubler DJ. 2011. Dengue, Urbanization and Globalization: The Unholy Trinity of the 21st Century. *Tropical*
518 *Medicine and Health* 39:S3–S11. DOI: 10.2149/tmh.2011-s05.

519 Heitmann A, Jansen S, Lühken R, Leggewie M, Schmidt-Chanasit J, Tannich E. 2018. Forced Salivation As a
520 Method to Analyze Vector Competence of Mosquitoes. *Journal of Visualized Experiments : JoVE*:57980.
521 DOI: 10.3791/57980.

522 Hurk AF van den, Hall-Mendelin S, Pyke AT, Smith GA, Mackenzie JS. 2010. Vector Competence of
523 Australian Mosquitoes for Chikungunya Virus. *Vector-Borne and Zoonotic Diseases* 10:489–495. DOI:
524 10.1089/vbz.2009.0106.

525 Islam ZU, Bishop SC, Savill NJ, Rowland RRR, Lunney JK, Trible B, Doeschl-Wilson AB. 2013. Quantitative
526 Analysis of Porcine Reproductive and Respiratory Syndrome (PRRS) Viremia Profiles from Experimental
527 Infection: A Statistical Modelling Approach. *PLoS ONE* 8:e83567. DOI: 10.1371/journal.pone.0083567.

528 Kraemer MUG, Reiner RC, Brady OJ, Messina JP, Gilbert M, Pigott DM, Yi D, Johnson K, Earl L, Marczak
529 LB, Shirude S, Weaver ND, Bisanzio D, Perkins TA, Lai S, Lu X, Jones P, Coelho GE, Carvalho RG, Bortel
530 WV, Marsboom C, Hendrickx G, Schaffner F, Moore CG, Nax HH, Bengtsson L, Wetter E, Tatem AJ,
531 Brownstein JS, Smith DL, Lambrechts L, Cauchemez S, Linard C, Faria NR, Pybus OG, Scott TW, Liu Q,
532 Yu H, Wint GRW, Hay SI, Golding N. 2019. Past and future spread of the arbovirus vectors Aedes aegypti
533 and Aedes albopictus. *Nature Microbiology* 4:854–863. DOI: 10.1038/s41564-019-0376-y.

534 Labadie K, Larcher T, Joubert C, Mannioui A, Delache B, Brochard P, Guigand L, Dubreil L, Lebon P, Verrier
535 B, Lamballerie X de, Suhrbier A, Cherel Y, Grand RL, Roques P. 2010. Chikungunya disease in nonhuman
536 primates involves long-term viral persistence in macrophages. *Journal of Clinical Investigation* 120:894–
537 906. DOI: 10.1172/jci40104.

538 Labeaud AD, Bashir F, King CH. 2011. Measuring the burden of arboviral diseases: the spectrum of morbidity
539 and mortality from four prevalent infections. *Population Health Metrics* 9:1. DOI: 10.1186/1478-7954-9-1.

540 Lambrechts L. 2011. Quantitative genetics of Aedes aegypti vector competence for dengue viruses: towards a
541 new paradigm? *Trends in Parasitology* 27:111–114. DOI: 10.1016/j.pt.2010.12.001.

542 Lanciotti RS, Kosoy OL, Laven JJ, Panella AJ, Velez JO, Lambert AJ, Campbell GL. 2007. Chikungunya virus
543 in US travelers returning from India, 2006. *Emerging Infectious Diseases* 13:764–767. DOI:
544 10.3201/eid1305.070015.

545 Laurent P, Roux KL, Grivard P, Bertil G, Naze F, Picard M, Staikowsky F, Barau G, Schuffenecker I, Michault
546 A. 2007. Development of a sensitive real-time reverse transcriptase PCR assay with an internal control to
547 detect and quantify chikungunya virus. *Clinical Chemistry* 53:1408–1414. DOI:
548 10.1373/clinchem.2007.086595.

549 Lequime S, Bastide P, Dellicour S, Lemey P, Baele G. 2020a. nosoi: A stochastic agent-based transmission
550 chain simulation framework in r. *Methods in Ecology and Evolution* 11:1002–1007. DOI: 10.1111/2041-
551 210x.13422.

552 Lequime S, Dehecq J-S, Matheus S, Laval F de, Almeras L, Briolant S, Fontaine A. 2020b. Modeling intra-
553 mosquito dynamics of Zika virus and its dose-dependence confirms the low epidemic potential of Aedes
554 albopictus. *PLOS Pathogens* 16:e1009068. DOI: 10.1371/journal.ppat.1009068.

555 Mayton EH, Hernandez HM, Vitek CJ, Christofferson RC. 2021. A Method for Repeated, Longitudinal
556 Sampling of Individual Aedes aegypti for Transmission Potential of Arboviruses. *Insects* 12:292. DOI:
557 10.3390/insects12040292.

558 Merwaiss F, Filomatori CV, Susuki Y, Bardossy ES, Alvarez DE, Saleh M-C. 2020. "Chikungunya virus
559 replication rate determines the capacity of crossing tissue barriers in mosquitoes." *Journal of Virology* 95.
560 DOI: 10.1128/jvi.01956-20.

561 Messaoudi I, Vomaske J, Totonchy T, Kreklywich CN, Haberthur K, Springgay L, Brien JD, Diamond MS,
562 DeFilippis VR, Streblow DN. 2013. Chikungunya Virus Infection Results in Higher and Persistent Viral
563 Replication in Aged Rhesus Macaques Due to Defects in Anti-Viral Immunity. *PLoS Neglected Tropical*
564 *Diseases* 7:e2343. DOI: 10.1371/journal.pntd.0002343.

565 Moloney RM, Kmush B, Rudolph KE, Cummings DAT, Lessler J. 2014. Incubation Periods of Mosquito-Borne
566 Viral Infections: A Systematic Review. *The American Journal of Tropical Medicine and Hygiene* 90:882–
567 891. DOI: 10.4269/ajtmh.13-0403.

568 Nguyet MN, Duong THK, Trung VT, Nguyen THQ, Tran CNB, Long VT, Dui LT, Nguyen HL, Farrar JJ,
569 Holmes EC, Rabaa MA, Bryant JE, Nguyen TT, Nguyen HTC, Nguyen LTH, Pham MP, Nguyen HT, Luong
570 TTH, Wills B, Nguyen CVV, Wolbers M, Simmons CP. 2013. Host and viral features of human dengue
571 cases shape the population of infected and infectious Aedes aegypti mosquitoes. *Proceedings of the National*
572 *Academy of Sciences of the United States of America* 110:9072–9077. DOI: 10.1073/pnas.1303395110.

573 Panning M, Grywna K, Esbroeck M van, Emmerich P, Drosten C. 2008. Chikungunya fever in travelers
574 returning to Europe from the Indian Ocean region, 2006. *Emerging Infectious Diseases* 14:416–422. DOI:
575 10.3201/eid1403.070906.

576 Paupy C, Delatte H, Bagny L, Corbel V, Fontenille D. 2009. Aedes albopictus, an arbovirus vector: from the
577 darkness to the light. *Microbes and Infection / Institut Pasteur* 11:1177–1185. DOI:
578 10.1016/j.micinf.2009.05.005.

579 Raquin V, Merkling SH, Gausson V, Moltini-Conclois I, Frangeul L, Varet H, Dillies M-A, Saleh M-C,
580 Lambrechts L. 2017. Individual co-variation between viral RNA load and gene expression reveals novel host
581 factors during early dengue virus infection of the Aedes aegypti midgut. *PLoS Neglected Tropical Diseases*
582 11:e0006152. DOI: 10.1371/journal.pntd.0006152.

583 Raquin V, Moro CV, Saucereau Y, Tran F-H, Potier P, Mavingui P. 2015. Native Wolbachia from Aedes
584 albopictus Blocks Chikungunya Virus Infection In Cellulo. *PLOS ONE* 10:e0125066. DOI:
585 10.1371/journal.pone.0125066.

586 Rezza G, Nicoletti L, Angelini R, Romi R, Finarelli A, Panning M, Cordioli P, Fortuna C, Boros S, Magurano F,
587 Silvi G, Angelini P, Dottori M, Ciufolini M, Majori G, Cassone A, group for the C study. 2007. Infection
588 with chikungunya virus in Italy: an outbreak in a temperate region. *The Lancet* 370:1840–1846. DOI:
589 10.1016/s0140-6736(07)61779-6.

590 Riswari SF, Ma'roef CN, Djauhari H, Kosasih H, Perkasa A, Yudhaputri FA, Artika IM, Williams M, Ven A
591 van der, Myint KS, Alisjahbana B, Ledermann JP, Powers AM, Jaya UA. 2015. Study of viremic profile in
592 febrile specimens of chikungunya in Bandung, Indonesia. *Journal of clinical virology : the official*
593 *publication of the Pan American Society for Clinical Virology* 74:61–5. DOI: 10.1016/j.jcv.2015.11.017.

594 Sanchez-Vargas I, Harrington LC, Black WC, Olson KE. 2019. Analysis of Salivary Glands and Saliva from
595 Aedes albopictus and Aedes aegypti Infected with Chikungunya Viruses. *Insects* 10:39. DOI:
596 10.3390/insects10020039.

597 Schuffenecker I, Iteman I, Michault A, Murri S, Frangeul L, Vaney M-C, Lavenir R, Pardigon N, Reynes J-M,
598 Pettinelli F, Biscornet L, Diancourt L, Michel S, Duquerroy S, Guigon G, Frenkiel M-P, Bréhin A-C, Cubito
599 N, Desprès P, Kunst F, Rey FA, Zeller H, Brisse S. 2006. Genome Microevolution of Chikungunya Viruses
600 Causing the Indian Ocean Outbreak. *PLoS Medicine* 3:e263. DOI: 10.1371/journal.pmed.0030263.

601 Sherpa S, Blum MGB, Capblancq T, Cumer T, Rioux D, Després L. 2019. Unravelling the invasion history of
602 the Asian tiger mosquito in Europe. *Molecular Ecology* 28:2360–2377. DOI: 10.1111/mec.15071.

603 Smith DL, Battle KE, Hay SI, Barker CM, Scott TW, McKenzie FE. 2012. Ross, Macdonald, and a Theory for
604 the Dynamics and Control of Mosquito-Transmitted Pathogens. *PLoS Pathogens* 8:e1002588. DOI:
605 10.1371/journal.ppat.1002588.

606 Succo T, Leparc-Goffart I, Ferré J-B, Roiz D, Broche B, Maquart M, Noel H, Catelinois O, Entezam F, Caire D,
607 Jourdain F, Esteve-Moussion I, Cochet A, Paupy C, Rousseau C, Paty M-C, Golliot F. 2016. Autochthonous
608 dengue outbreak in Nîmes, South of France, July to September 2015. *Eurosurveillance* 21. DOI:
609 10.2807/1560-7917.es.2016.21.21.30240.

610 Tsetsarkin KA, Vanlandingham DL, McGee CE, Higgs S. 2007. A single mutation in chikungunya virus affects
611 vector specificity and epidemic potential. *PLoS pathogens* 3:e201. DOI: 10.1371/journal.ppat.0030201.

612 Vazeille M, Moutailler S, Coudrier D, Rousseaux C, Khun H, Huerre M, Thiria J, Dehecq J-S, Fontenille D,
613 Schuffenecker I, Despres P, Failloux A-B. 2007. Two Chikungunya Isolates from the Outbreak of La
614 Reunion (Indian Ocean) Exhibit Different Patterns of Infection in the Mosquito, Aedes albopictus. *PLoS*
615 *ONE* 2:e1168. DOI: 10.1371/journal.pone.0001168.

616 Vega-Rua A, Zouache K, Caro V, Diancourt L, Delaunay P, Grandadam M, Failloux A-B. 2013. High
617 Efficiency of Temperate Aedes albopictus to Transmit Chikungunya and Dengue Viruses in the Southeast of
618 France. *PLoS ONE* 8:e59716. DOI: 10.1371/journal.pone.0059716.

619 Vega-Rua A, Zouache K, Girod R, Failloux A-B, Lourenco-de-Oliveira R. 2014. High Level of Vector
620 Competence of Aedes aegypti and Aedes albopictus from Ten American Countries as a Crucial Factor in the
621 Spread of Chikungunya Virus. *Journal of Virology* 88:6294–6306. DOI: 10.1128/jvi.00370-14.

622 Venturi G, Luca MD, Fortuna C, Remoli ME, Riccardo F, Severini F, Toma L, Manso MD, Benedetti E,
623 Caporali MG, Amendola A, Fiorentini C, Liberato CD, Giammattei R, Romi R, Pezzotti P, Rezza G, Rizzo
624 C. 2017. Detection of a chikungunya outbreak in Central Italy, August to September 2017. *Eurosurveillance*
625 22:17–00646. DOI: 10.2807/1560-7917.es.2017.22.39.17-00646.

626 Viglietta M, Bellone R, Blisnick AA, Failloux A-B. 2021. Vector Specificity of Arbovirus Transmission.
627 *Frontiers in Microbiology* 12:773211. DOI: 10.3389/fmicb.2021.773211.

628 Wickham H, Averick M, Bryan J, Chang W, McGowan L, François R, Grolemund G, Hayes A, Henry L, Hester
629 J, Kuhn M, Pedersen T, Miller E, Bache S, Müller K, Ooms J, Robinson D, Seidel D, Spinu V, Takahashi K,
630 Vaughan D, Wilke C, Woo K, Yutani H. 2019. Welcome to the Tidyverse. *Journal of Open Source Software*
631 4:1686. DOI: 10.21105/joss.01686.

632 Zouache K, Fontaine A, Vega-Rua A, Mousson L, Thiberge J-M, Lourenco-De-Oliveira R, Caro V, Lambrechts
633 L, Failloux A-B. 2014. Three-way interactions between mosquito population, viral strain and temperature
634 underlying chikungunya virus transmission potential. *Proceedings of the Royal Society B: Biological*
635 *Sciences* 281:20141078. DOI: 10.1098/rspb.2014.1078.

636